



Contents lists available at ScienceDirect

Biomaterials

journal homepage: www.elsevier.com/locate/biomaterials

Tuning the non-equilibrium state of a drug-encapsulated poly(ethylene glycol) hydrogel for stem and progenitor cell mobilization

Youyun Liang^{a,g}, Tor W. Jensen^c, Edward J. Roy^d, Chaenyung Cha^b, Ross J. DeVolder^a, Richie E. Kohman^b, Bao Zhong Zhang^a, Kyle B. Textor^c, Lauretta A. Rund^e, Lawrence B. Schook^f, Yen Wah Tong^{g,h}, Hyunjoon Kong^{a,c,*}

^aDepartment of Chemical and Biomolecular Engineering, University of Illinois, Urbana-Champaign, Urbana, IL 61801, USA

^bDepartment of Chemistry, University of Illinois, Urbana-Champaign, Urbana, IL 61801, USA

^cInstitute of Genomic Biology, University of Illinois, Urbana-Champaign, Urbana, IL 61801, USA

^dNeuroscience Program and Department of Pathology, University of Illinois, Urbana-Champaign, Urbana, IL 61801, USA

^eDepartment of Animal Sciences, University of Illinois, Urbana-Champaign, Urbana, IL 61801, USA

^fDivision of Biomedical Sciences and Laboratory of Comparative Genomics, University of Illinois, Urbana-Champaign, Urbana, IL 61801, USA

^gDepartment of Chemical and Biomolecular Engineering, National University of Singapore, 117576, Singapore

^hDivision of Bioengineering, National University of Singapore, 117576, Singapore

ARTICLE INFO

Article history:

Received 14 September 2010

Accepted 14 November 2010

Available online xxx

Keywords:

Michael-Addition

Poly(ethyleneimine)

Rigidity

Degradation rate

Granulocyte colony stimulating factor

(GCSF)

ABSTRACT

Injectable and biodegradable hydrogels have been increasingly studied for sustained drug delivery in various molecular therapies. However, it remains a challenge to attain desired delivery rate at injection sites due to local tissue pressures exerted on the soft hydrogels. Furthermore, there is often limited controllability of stiffness and degradation rates, which are key factors for achieving desired drug release rate and therapeutic efficacy. This study presents a stiff and metastable poly(ethylene glycol) diacrylate (PEGDA)-poly(ethyleneimine) (PEI) hydrogel which exhibits an elastic modulus equivalent to bulk plastic materials, and controllable degradation rate independent of its initial elastic modulus. Such unique stiffness was attained from the highly branched architecture of PEI, and the decoupled controllability of degradation rate was achieved by tuning the non-equilibrium swelling of the hydrogel. Furthermore, a single intramuscular administration of granulocyte colony stimulating factor (GCSF)-encapsulated PEGDA-PEI hydrogel extended the mobilization of mononuclear cells to four days. A larger yield of expanded CD34⁺ and CD31⁺ endothelial progenitor cells (EPCs) was also obtained as compared to the daily bolus administration. Overall, the hydrogel created in this study will be useful for the controlled and sustained delivery of a wide array of drug molecules.

© 2010 Elsevier Ltd. All rights reserved.

1. Introduction

Injectable and biodegradable hydrogels have been increasingly studied as drug carriers for encapsulation, transport and release of growth factors and cytokines in various molecular therapies such as stem cell mobilization therapy. Stem cell mobilization, developed to augment bone marrow and regenerate tissue, has often been implemented by repeated administration of cytokines e.g. granulocyte colony stimulating factor (GCSF), for periods of three to six days [1–3]. Since the half-life of GCSF is about 3.5 hours, it is necessary to administer GCSF on a daily basis[4]. To circumvent the necessity of repeated drug administration and potentially

accompanying complications, local injection of GCSF-encapsulated hydrogels into skeletal muscle was previously attempted[5].

For successful use of hydrogels in such application, the GCSF-encapsulated hydrogel should initially present stiffness high enough to maintain its structural integrity, so as to sequester the GCSF at the injected site. In addition, the hydrogel should degrade in a controlled manner, independent of its initial stiffness for sustained release of the encapsulated GCSF. However, conventional hydrogel systems used for drug delivery are often plagued by limited controllability of stiffness and an inverse dependency of degradation rate on the initial rigidity[6,7]. Previously, certain efforts were made to develop structurally rigid hydrogel systems. These include double network hydrogels, topological gels, nano-composite gels and cryogels, all of which designed to exhibit elastic moduli comparable to hard cartilage tissues[8–12]. However, these hydrogels typically had limited degradation rates which precluded their use as drug-releasing carriers.

* Corresponding author. Department of Chemical and Biomolecular Engineering, University of Illinois, Urbana-Champaign, Urbana, IL 61801, USA.

E-mail address: hjkong06@illinois.edu (H. Kong).

We hypothesized that the cross-linking of a polymer carrying multiple reactive groups along a hyper-branched architecture would generate a highly rigid hydrogel system. In addition, incorporation of charged groups in the hydrogel would tune osmotic water influx and subsequently allow the control of degradation rates with the number of charged groups present. We examined this hypothesis by cross-linking PEGDA and hyper-branched PEI. The branched architecture of PEI would increase the gel rigidity and unreacted amines would drive the non-equilibrium swelling of the hydrogel. The stiffness and degradation rate of the PEGDA-PEI hydrogel, tuned with mass fraction of PEGDA and PEI, were characterized by measuring elastic modulus and swelling ratio of the hydrogel. The mechanism underlying hydrogel degradation was also studied by monitoring water diffusion into the hydrogel using magnetic resonance imaging (MRI) and also by altering the ionic strength of the incubation media of the hydrogel. Furthermore, the drug release profile of hydrogel was examined both *in vitro* and *in vivo* using fluorescent proteins. Ultimately, GCSF-encapsulated hydrogel was intramuscularly injected into a pig to evaluate the performance of the PEGDA-PEI hydrogel in mobilizing clinically relevant stem cell populations into circulation.

2. Experimental

2.1. Synthesis of hydrogels

To prepare the PEGDA-PEI hydrogels, aqueous solutions of PEGDA (molecular weight (M_w) \approx 400, Polysciences) and PEI ($M_w \approx$ 2000, Sigma-Aldrich) were thoroughly mixed. Then, the mixture was placed between two glass plates with a spacer of 1 mm. Following incubation at room temperature for 2 min, the hydrogel disks were punched out using punchers with diameters of 5 or 10 mm. For certain experiments where the hydrogel was injected into a mouse or pig, the mixture of PEGDA and PEI was loaded in a syringe for injection into the target tissue before gelation. Both PEI with branched architecture and linear architecture were used. Pure PEGDA hydrogels were also formed by mixing aqueous solutions of PEGDA with 0.01% Irgacure 2959 (Sigma-Aldrich) and subsequently exposing the PEGDA solutions to UV light for 10 min. The ^1H NMR spectra of polymer precursors, fragments, and the resultant hydrogels were collected using NMR (500 MHz, Varian).

2.2. Measurements of elastic modulus and swelling ratio of hydrogels

The elastic modulus (E_0) of a hydrogel disk was measured by compressing the disks with a mechanical testing system (MTS Insight) at a rate of 1 mm/min and measuring the resulting stress. E_0 was determined from the slope of the linear curve between stress and strain at the first 10% of the strain. The initial swelling ratios of the hydrogels (Q_0) were also quantified with the ratios between the mass of the hydrogel disks and that of the lyophilized hydrogels. The initial number of cross-links (N_0) was further calculated using Eq. (1) and Eq. (2) according to rubber elasticity theory [6]:

$$N_0 = \frac{SQ^{-\frac{1}{3}}}{RT} \quad (1)$$

where S is the shear modulus calculated from the slope of stress versus (λ^{-2} - λ) assuming the hydrogels followed an affined network model (λ : ratio of deformed height to original height) and Q is the degree of swelling calculated from Eq. (2).

$$Q = v^{-2} = \rho_p \left[\frac{Q_0}{\rho_s} + \frac{1}{\rho_p} \right] \quad (2)$$

where ρ_s is the density of water, and ρ_p is the density of polymer.

Hydrogels were incubated in 1 ml PBS (pH 7.4), and their changes in swelling ratios were recorded by measuring their masses until the disks were completely disintegrated. The swelling ratio at time, t , (Q_m) was normalized by the initial swelling ratio of the disks (Q_0). In parallel, the change in solid mass of the hydrogel disks during incubation in PBS was also monitored by measuring the dried solid mass of the hydrogels at various time points following the lyophilization.

The increase in Q_m of the hydrogel over time was further fitted to Peppas's model to calculate its degradation rate (k_1) and swelling exponent (n) [13,14].

$$\frac{Q_m - Q_0}{Q_0} = k_1 t^n \quad (3)$$

where Q_0 is the initial swelling ratio, Q_m is the swelling ratio of hydrogel disks at time, t (min).

The diffusivity (D) was further calculated from k_1 and n using Eq. (4) [15].

$$D = \pi r^2 \sqrt[n]{\frac{k_1}{4}} \quad (4)$$

where D is the diffusion coefficient of water in cm^2s^{-1} , r is the radius of the hydrogel disks in cm, and $k_1 = k_1(T)^n$, where T is the time expressed in seconds.

The number of unreacted amines after hydrogel formation was investigated by reaction with 2, 4, 6-trinitrobenzenesulfonic acid (TNBS) (Sigma-Aldrich). Briefly, hydrogel disks were degraded by reaction with 1 M sodium hydroxide (Sigma-Aldrich) to expose the unreacted amine groups. The number of unreacted amines remaining after PEGDA-PEI cross-linking was then determined by a 15 min-incubation with TNBS in the presence of sodium bicarbonate buffer (0.01 M, pH 8.5). At the end of the assay, the absorbance was measured at 335 nm with a microplate reader (Synergy HT Multi-Mode Microplate Reader, Biotek Instruments), and the absorbance was converted to the number of unreacted amines using a calibration curve generated with different concentrations of PEI.

2.3. Imaging of water diffusion into hydrogels using magnetic resonance imaging (MRI)

Imaging of water diffusion through hydrogel disks was carried out using 600 MHz Varian Unity/Inova nuclear magnetic resonance (NMR) spectrometer (14.1 T magnet) at room temperature [16–18]. The maximum strength of the magnetic field gradient was 90 G cm^{-1} . Each hydrogel disk (10 mm in diameter, 1 mm in thickness) was incubated in deionized water. Then, the cross-sectional images of hydrogel disks through the middle were taken every 25 min by placing the swollen hydrogels in glass bottles which were inserted into a Radio Frequency (RF) coil for the measurements. Spin echo multi-slice (SEMS) pulse sequence was used to acquire resonance data, which were then converted into water density maps using VNMR 6.1C software. For SEMS pulse sequence, the repetition time (T_R) of 2 s and the echo time (T_E) of 10 ms were used. The field of view (FOV) was $1.5 \times 1.5 \text{ cm}$ with the slice thickness of 1 mm, and the image matrix was 256×256 pixels. After acquiring the images, colors were added to the images to visualize the water density spectrum using ImageJ (National Institutes of Health, <http://rsbweb.nih.gov/ij/>).

2.4. In vivo toxicity assay

Toxicity of the PEGDA-PEI hydrogels was evaluated by implanting them on the CAMs of chicken embryos [19]. Fertilized chicken eggs (Hy-Line W-36) were purchased from the Poultry Research Farm at the University of Illinois (Urbana, IL). The eggs were incubated at 37°C with 5% CO_2 . On the 8th day of gestation, a small hole ($1 \text{ cm} \times 1 \text{ cm}$) was created on top of each eggshell. After an additional day of incubation to acclimatize the embryos, different hydrogel disks (5 mm diameter, 1 mm thickness) were implanted on top of the CAMs (5 eggs per condition). After incubation for seven days, the membranes were fixed with 10% neutral buffered formalin (NBF) for 20 h. The fixed membrane surrounding the gel disk ($10 \text{ mm} \times 10 \text{ mm}$) was cut out. The collected tissue was processed for paraffin embedding, and the cross-sections were stained with standard Hematoxylin & Eosin (H&E) for histological analysis.

2.5. Measurement of the in vitro protein release rate

Fluorescent bovine serum albumin (BSA) (Invitrogen) was mixed with the aqueous PEI solutions prior to the cross-linking reaction with the PEGDA solutions. Hydrogel disks with diameters of 5 mm were punched out and incubated in phosphate buffered saline (PBS, pH 7.4) at 37°C . The PBS was exchanged with fresh media on a daily basis until the hydrogel disk was disintegrated. The fluorescence intensity from the BSA was measured with a microplate reader (Synergy HT Multi-Mode Microplate Reader, Biotek Instruments), and the amount of BSA released was back-calculated from the intensity using a calibration curve. The masses of the BSA released following the initial lag period was further converted to the release rate (k_2) and release exponent (m) using Ritger–Peppas equation [13].

$$\frac{M_t}{M_\infty} = k_2 t^m \quad (5)$$

where M_t is the cumulative amount of BSA released at time t , M_∞ is the total amount of BSA released, k_2 is the release constant, and m is the release exponent.

2.6. Analysis of the in vivo protein release

BSA was labeled with fluorescent IRDye[®] 800CW N-hydroxysuccinimide ester (Li-cor Biosciences) according to the instructions provided in the IRDye Protein Labeling Kit (Li-cor Biosciences). 30 μl of the mixture of fluorescent BSA and PBS or 30 μl of the fluorescent BSA-encapsulated PEGDA-PEI pre-gel solution (i.e. 12.5% PEGDA and 10% PEI) was injected into the back of mice (3 months old female C57BL/6 mice). The mice were anesthetized at different time points, and the injection sites and ears of the mice were imaged with the Odyssey Infrared Imaging System with Mousepod (Li-cor Biosciences). The fluorescent intensities of the BSA in all the mice were processed using the same settings. The fluorescence images were further superimposed with photos of the actual mice for clearer visualization. All

procedures on mice were performed with approval from the University of Illinois Institutional Animal Care and Use Committee (IACUC).

2.7. Stem cell mobilization study

The synthesized porcine GCSF was dissolved in PBS or encapsulated in hydrogels before delivery into pigs (3 month old female white landrace pigs weighing approximately 30 kg each) via intramuscular injection. The production procedure of porcine GCSF is described in the supplementary information. Conditions tested in this experiment included (i) single bolus injection of 3 mL PBS containing 1.2 mg of GCSF (number of samples was one), (ii) daily bolus injections of injection of 3 mL PBS containing 0.3 mg of GCSF (number of sample was one), (iii) single injection of 3 mL blank PEGDA-PEI hydrogel i.e. 20% PEGDA and 3.5% PEI (number of sample was one), and (iv) single injection of 3 mL of PEG-PEI hydrogel containing 1.2 mg of GCSF (number of sample was three). Blood samples were taken daily from the brachiocephalic vein by atraumatic venipuncture and collected directly into EDTA-containing vacutainer tubes. Cell counts of the non-erythrocyte fraction were performed on a Beckman Coulter AcT10 hematology analyzer (Beckman Coulter). At the end of the experiment, animals were sedated with a telozal-xylazine-ketamine cocktail and euthanized by an intravenous overdose injection of sodium pentobarbital. All procedures on pigs were performed with approval from the University of Illinois Institutional Animal Care and Use Committee (IACUC).

2.8. Analysis of mobilized cells

Mononuclear cells (MNCs) from the collected blood were isolated by density gradient centrifugation over Histopaque-1077 (Sigma–Aldrich) according to manufacturer's protocol. Isolated MNCs were re-suspended in complete endothelial growth medium (EGM-2; Lonza). After re-suspension, 5×10^6 cells/cm² were plated on a 24-well fibronectin coated plate (BD Biosciences). The cells were cultured for four days at 37 °C in a humidified 5% CO₂ incubator. After four days, non-adherent cells were removed by rinsing with PBS and fresh EGM-2 was added to the wells. Medium was changed every two to three days between passages. Flow cytometry was performed on the third passage to determine expression of markers CD34 and CD31. Cells were washed thrice with PBS containing 1% BSA (all subsequent washing steps were conducted in the same manner), incubated with primary anti-porcine CD34 antibody for 40 min at 4 °C and washed again. Following which, cells were then incubated with a phycoerythrin conjugated secondary antibody (Invitrogen) for 40 min at 4 °C, washed and incubated with a fluorescein isothiocyanate conjugated anti-porcine CD31 antibody (AbD) for 40 min at 4 °C before the final washing step. Stained cells were measured using a BD Biosciences LSRII flow cytometer using isotype control-stained cells to set negative regions.

3. Results and discussion

3.1. Stiff PEGDA-PEI hydrogel

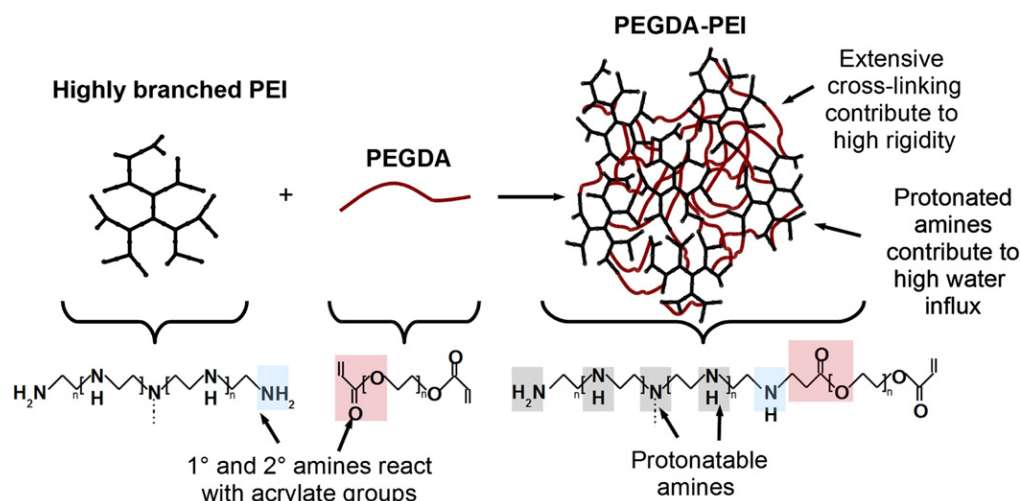
Hydrogels consisting of PEGDA and PEI, termed as PEGDA-PEI hydrogels, were formed through Michael reactions between PEGDA and branched PEI (Scheme 1). The hydrogels were formed within

1 min after the PEGDA and PEI were mixed together. The Michael reaction between the acrylate groups of PEGDA and the amine groups of PEI was confirmed by the disappearance of acrylate peaks at 6.2 ppm in the ¹H NMR spectra of the hydrogel and the disintegrated hydrogel fragments (Fig. S1). In contrast, mixtures of PEGDA and linear PEI did not form a hydrogel at similar concentrations [20]. Previously, certain studies reported the use of Michael reaction between PEGDA and PEI to prepare polymeric gene carriers in the form of nanoparticles [21,22]. However, this is the first study in which the Michael reaction between PEGDA and PEI is used to form a bulk hydrogel.

The load-bearing capacities of the resulting hydrogels were evaluated by measuring the compressive elastic moduli of the hydrogels formed with varied concentrations of PEGDA and PEI. The initial compressive moduli (E_0) of the PEGDA-PEI hydrogels were significantly increased with increasing concentrations of PEI at a constant PEGDA concentration of 20% or with increasing concentrations of PEGDA at a constant PEI concentration of 10% (Fig. 1). Overall, E_0 of the PEGDA-PEI hydrogels were controlled from 1 to 8 MPa, which are one to two orders of magnitude higher than elastic moduli of the pure PEGDA hydrogels formed from a radical cross-linking reaction (Fig. 1). Strikingly, E_0 of the hydrogels consisting of 20% PEGDA and 5–10% PEI were comparable to the compressive modulus of poly(styrene) (~4 MPa) as provided by American Society for Testing Materials (ASTM). The initial number of cross-links (N_0) for the PEGDA-PEI hydrogels, calculated from E_0 and the initial swelling ratios (Q_0) using rubber elasticity theory [Eq. (1) in the experimental section], was one order of magnitude higher than that of the pure PEGDA hydrogels formed from radical cross-linking reactions (Table S1).

3.2. Decoupled control of stiffness and degradation of PEGDA-PEI hydrogel

In parallel, degradation rates of the PEGDA-PEI hydrogels incubated in neutral phosphate buffered saline (PBS) were quantified by measuring the increase in swelling ratio (Q_m) over time. Initially, the swelling ratio increased without a decrease in solid mass. However, as the swelling ratios reached higher values of about 10, the solid mass of the hydrogel disks started to decrease significantly (Fig. S2). Interestingly, the time required for complete structural disintegration of the hydrogels decreased with increasing concentrations of



Scheme 1. PEGDA-PEI hydrogels were formed by Michael-type cross-linking reactions between the amine groups of branched PEI and the acrylate groups of PEGDA.

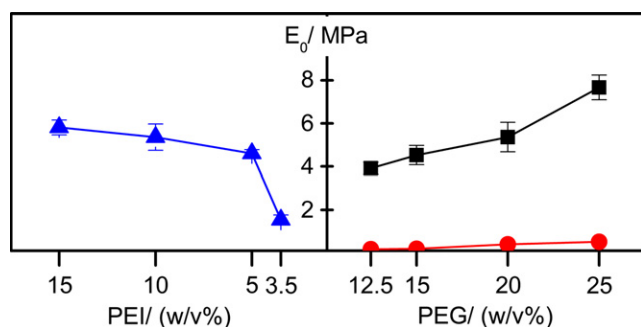


Fig. 1. Tuning stiffness of the PEGDA-PEI hydrogels. Initial compressive elastic moduli (E_0) of the PEGDA-PEI hydrogels were increased with PEI concentration at a given PEGDA concentration of 20% (▲ in the left plot). E_0 of the PEGDA-PEI hydrogels were also increased with PEGDA concentration at a given PEI concentration of 10% (■ in the right plot), and the dependency of E_0 on the PEGDA concentration was more significant than the radically crosslinked PEGDA hydrogels (● in the right plot). The E_0 value and error bar for each condition represent the average elastic modulus and the standard deviation from the measurements of four samples.

PEI at a constant PEGDA concentration of 20%, or with decreasing concentrations of PEGDA at a constant PEI concentration of 10%. The dependency of Q_m on incubation time was fitted to calculate the degradation rate (k_1), swelling exponent (n) and water diffusivity (D) [Fig. 2a & Eqs. (3) and (4) in the experimental section] [13–15]. Increasing the PEI concentration at a constant PEGDA concentration of 20% increased k_1 , n , and D (Fig. 2a and Table 1). In contrast, increasing the PEGDA concentration at a constant PEI concentration

of 10% significantly decreased k_1 , n and D (Fig. 2b and Table 1). These changes in k_1 , n , and D , resulting from changes in PEGDA concentrations or PEI concentrations, were related to the number of unreacted amine groups of PEI (Fig. 2c and Table 1). Overall, increasing the PEGDA concentration at a constant PEI concentration resulted in an inverse dependency between D and E_0 , typical of conventional hydrogels. Conversely, increasing the PEI concentration at a constant PEGDA concentration resulted in increases of both D and E_0 of the hydrogel, which is distinct from conventional biodegradable hydrogels (Fig. 2d).

The degradation process of the PEGDA-PEI hydrogel was further examined with MRI, which enabled the visualization of water protons that were bound to (“bound water”), and free from (“free water”) the hydrogels (Fig. 3) [16]. It has been demonstrated that “bound water” presents much stronger signal intensity than “free water” [16]. Following imaging of the hydrogels, the resonance intensities in the MRI was converted to the color density map as shown in the scale bar (Fig. 3). The pure PEGDA hydrogel undergoing swelling in PBS showed a gradual increase of “bound water” volume as confirmed with the increase of yellow color intensity. In contrast, the PEGDA-PEI hydrogel which rapidly swelled in PBS showed an initial increase in volume of “bound water” followed by the increase of the “free water” volume, as exhibited by the increase and subsequent decrease of yellow color intensity. The increase of the “free water” demonstrated the much higher water diffusivities in PEGDA-PEI hydrogels as compared to pure PEGDA hydrogels. The rate of increase in the “free water” volume became larger with an increase in PEI concentration, which illustrated that the PEI drove

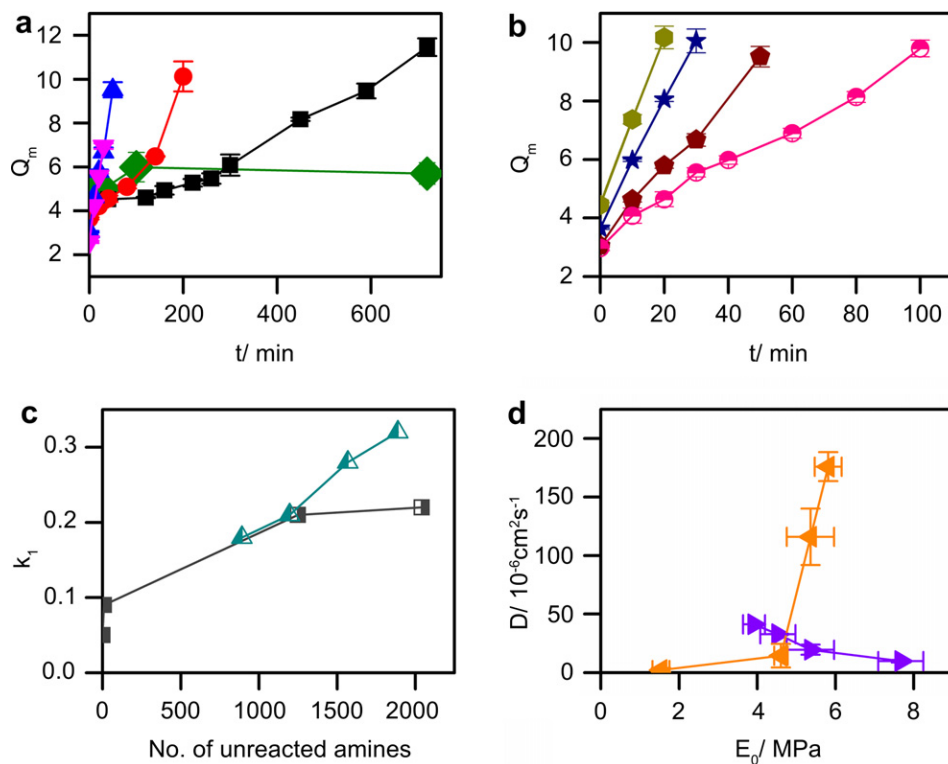


Fig. 2. Tuning degradation rates of the PEGDA-PEI hydrogels (a) The normalized swelling ratios (Q_m) of the hydrogels were increased over time, and the dependency of Q_m on time was modulated by the PEI concentration. Q_m was quantified by dividing the swelling ratio of the hydrogel at a certain time, t , by the initial swelling ratio (Q_0) of the hydrogel. The PEI concentration was increased from 3.5% (■) to 5% (●), 10% (▲) and 15% (▼) at a given PEGDA concentration of 20%. The radically crosslinked 20% PEGDA (◆) hydrogel presented relatively constant Q_m . (b) The dependency of Q_m on time was also modulated by the PEGDA concentration which was increased from 12.5% (●), to 15% (★), 20% (●) and 25% (●) at a given PEI concentration of 10%. (c) Degradation rates (k_1) were increased with the number of unreacted amines, which were varied with PEI concentrations (■) or PEGDA concentrations (▲) of the PEGDA-PEI hydrogels. (d) Increasing the PEI concentration of the hydrogels at a given PEGDA concentration of 20% resulted in the increase of both E_0 and D (▲). In contrast, increasing the PEGDA concentration of the hydrogels at a given PEI concentration of 10% led to the inverse dependency between D and E_0 (●).

Table 1

The swelling constants (k_1), swelling exponents (n) and water diffusion coefficients (D), for different hydrogel formulations were determined from logarithmic plots of Q_m vs t [Eq. (3)] ($r^2 \geq 0.97$). k_1 , n and D decreased with increasing PEGDA concentration at a given PEI concentration of 10%, while they increased with increasing PEI concentration at a given PEGDA concentration of 20%. The moles of unreacted amines decreased with increasing PEGDA concentration at a given PEI concentration of 10% and the moles of unreacted amines increased with increasing PEI concentration at a given PEGDA concentration of 20%.

10% PEI					20% PEGDA				
PEGDA (%)	k_1	n	D ($10^{-5} \text{ cm}^2 \text{ s}^{-1}$)	Unreacted Amines (10^{-6} mol)	PEI (%)	k_1	n	D ($10^{-5} \text{ cm}^2 \text{ s}^{-1}$)	Unreacted Amines (10^{-6} mol)
12.5	0.32	0.97	94.8	1888	3.5	0.05	0.66	1.9	0
15	0.28	0.92	72.3	1569	5	0.09	0.83	7.0	9.4
20	0.21	0.86	42.8	1196	10	0.21	0.86	42.8	1249
25	0.18	0.78	23.3	892	15	0.22	0.92	49.2	2041

the faster structural disintegration of the hydrogel by facilitating the accumulation of “free water” in the hydrogel.

The degradation rates of the PEGDA-PEI hydrogels could also be tuned by extrinsic factors such as ionic strength of PBS. Interestingly, the rate of water uptake of the PEGDA-PEI hydrogel was decreased with increasing ionic strengths of the PBS (Table S2). Ultimately, increasing ionic strength of the PBS solution by 20 times induced the hydrogel's swelling to reach an equilibrium state during the first 4 days of incubation. These results suggest that increasing the ionic strength of PBS inhibited swelling of the hydrogel, likely because of the screening of the charged groups in PEI, and the elevation of osmotic efflux of water from the hydrogels.

The cytotoxicity and immunogenicity of the hydrogel fragments, resulting from the degradation process, were further examined by implanting hydrogel disks onto chicken chorioallantoic membranes (CAMs). The hydrogels implanted on CAMs degraded at a rate comparable to the hydrogels incubated in PBS. Hydrogels containing less than 15% PEI did not stimulate inflammation or present cytotoxicity (Fig. S3).

3.3. Drug release profile of PEGDA-PEI hydrogel

Next, the effects of PEI concentrations on drug release profiles were examined by encapsulating fluorescently labeled bovine serum albumin (BSA) into the hydrogel (Fig. 4a). The encapsulation of the BSA into the PEGDA-PEI hydrogel decreased the degradation rate of the hydrogel. It is likely that electrostatic attraction between negatively charged BSA and amine groups of PEI slowed the degradation rate of the hydrogel, because of the decrease in the effective number of protonated amine groups. However, the degradation rate of the hydrogel was still controlled by the concentration of PEI. Specifically, the BSA was released from the hydrogels following a lag period (t_1), which was extended from 1.0 to 6.5 days by decreasing the concentration of PEI (Table 2). The release rate of BSA (k_2), calculated using Eq. (5) in the experimental section, was also increased with the concentration of the PEI [13]. The dependency of k_2 on the degradation rate (k_1) of the hydrogels indicated that the drug release kinetics from the PEGDA-PEI hydrogel was controlled by the degradation behavior of the hydrogel. This result implied that

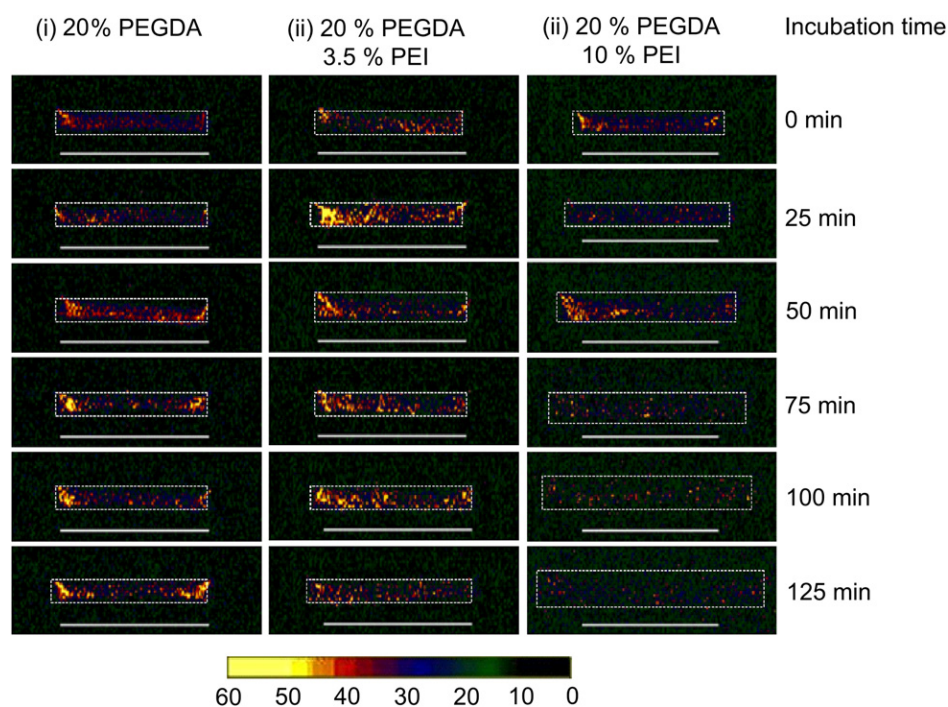


Fig. 3. Monitoring water diffusion using MRI. Water sorption processes into (i) a hydrogel solely consisting of 20% PEGDA, (ii) a hydrogel consisting of 20% PEGDA and 3.5% PEI, and (iii) a hydrogel consisting of 20% PEGDA and 10% PEI were monitored using MRI. The MRI images were taken every 25 min after incubating the gel in deionized water. White bars under the gel represent the original lengths of the hydrogels (10 mm). The dotted lines in the MRI images represent the periphery of the hydrogels. Scale bar on the bottom indicates the degree of interaction between water and hydrogels. A high intensity of yellow color denotes strongly “bound” water molecules, whereas a low intensity of yellow color corresponds to “free” water molecule. Pure PEGDA hydrogel (i) showed limited change of its original volume along with the gradual increase of the amount of “bound” water over time. In contrast, the PEGDA-PEI hydrogels (ii and iii) showed the rapid increase of “free” water volumes over time and, consequently, the drastic increase of the hydrogel volumes.

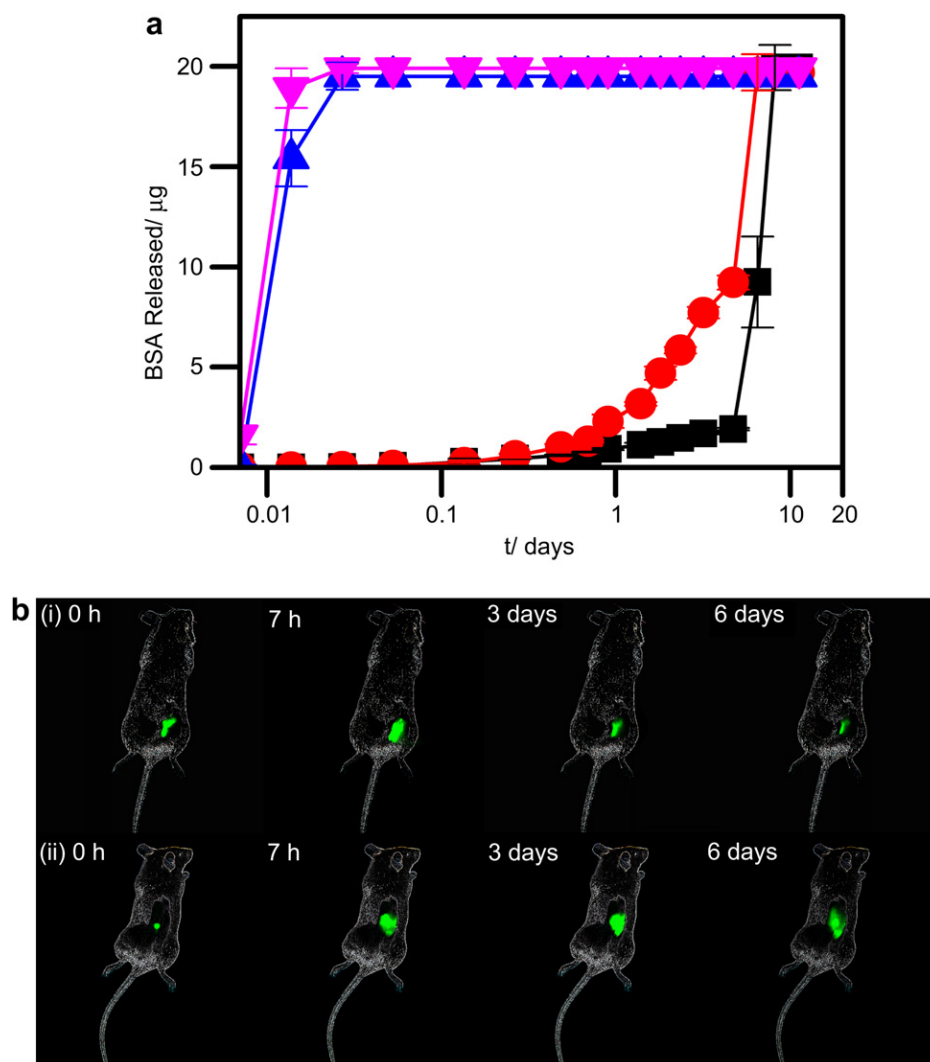


Fig. 4. Modulating the drug release rates of the hydrogels (a) The *in vitro* BSA release profiles from the PEGDA-PEI hydrogels were regulated by the concentrations of PEI. The PEI concentration was changed from 3.5% (■) to 5% (●), 10% (▲) and 15% (▼), while keeping the PEGDA concentration constant at 20%. (b) Bolus injection of the fluorescent BSA resulted in the rapid decrease of fluorescence at the injection site (photos in the upper row). In contrast, injection of the BSA-encapsulated hydrogel consisting of 12.5% PEGDA and 10% PEI led to the sustained fluorescence at the injection site over six days (photos in the lower row). Green fluorescence in the photos represents the fluorescent BSA.

degradation process of the hydrogel expanded the pores of the hydrogel and facilitated diffusion of BSA from the hydrogel.

In addition, the BSA-encapsulated PEGDA-PEI hydrogel was subcutaneously injected into mouse models to examine the role of the hydrogels in the displacement of BSA from the injection site *in vivo*. Unlike the *in vitro* studies, the initial elastic moduli of the hydrogels should also influence BSA's displacement along with the degradation rate, because of the tissue pressures exerted on the

hydrogels. In this study, hydrogels used consisted of 12.5% PEGDA and 10% PEI. These hydrogels had elastic moduli of approximately 4 MPa and degraded in less than a day in PBS solution. The fluorescent BSA administered via bolus injection dispersed rapidly, as confirmed with the rapid decrease of fluorescence at the injection site within three days (Fig. 4b). In contrast, injection of the BSA-encapsulated PEGDA-PEI hydrogels slowed the spread of the BSA at the injection site as shown by the slower decrease of fluorescence over six days. Subsequently, the PEGDA-PEI hydrogels resulted in a smaller rate of decrease in circulating BSA, demonstrated by the slower change of fluorescence in the mice's ears than bolus injection (Fig. S4). Coupled with the *in vitro* BSA release study, this result clearly demonstrates that the PEGDA-PEI hydrogel enabled the systemic and sustained delivery of BSA.

Table 2

The lag periods, quantified with time taken for 10% release of BSA (t_1), drug release constants (k_2), and release exponents (m) for different hydrogel formulations were determined from logarithmic plots of M_t/M_∞ vs t [Eq. (5)] ($r^2 \geq 0.74$). k_2 and m were regulated by the PEI concentrations at a given PEGDA concentration of 20%.

20% PEGDA			
PEI (%)	t_1 (days)	$\ln(k_2)$	m
3.5	6.27	-1.24	0.81
5	1.28	-0.21	0.92
10	0.01	11.03	2.15
15	0.01	13.3	2.17

3.4. Sustained stem cell mobilizing using GCSF-encapsulated PEGDA-PEI hydrogel

Lastly, GCSF was encapsulated into hydrogels consisting of 20% PEGDA and 3.5% PEI, which presented an initial elastic modulus of

3 MPa and released BSA more slowly than the hydrogel containing 10% PEI. As the GCSF with an isoelectric point between 5.8 and 6.6, would minimally interact with amine groups of PEI in a neutral condition, there would be insignificant decrease in the degradation rate of the hydrogel. The GCSF-encapsulated hydrogel was injected

into the shoulder muscle of porcine test animals, where the load-bearing capacity of the hydrogels would also influence the release profiles of the GCSF along with the degradation rate. The mixtures of PEGDA and PEI formed a stiff hydrogel right after injection of the pre-gel solution, similar to the gel formed *in vitro* (Fig. S5). Injection

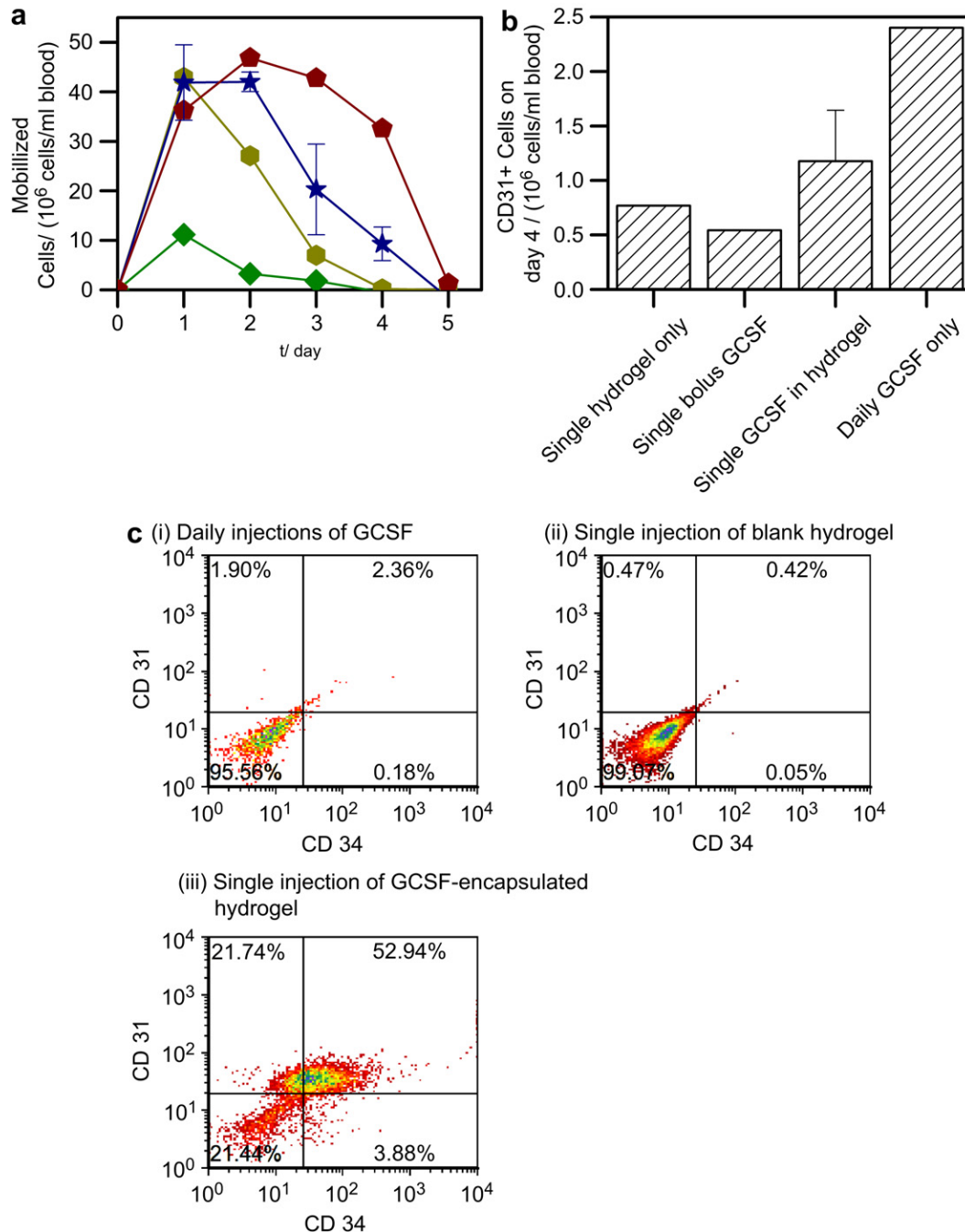


Fig. 5. GCSF-encapsulated PEGDA-PEI stem cell mobilization (a) GCSF solutions or GCSF-encapsulated PEGDA-PEI hydrogels were injected intramuscularly into pigs, and the number of mononuclear cells in the peripheral blood was monitored for four days. The graph represents the number of mononuclear cells over baseline during the course of the experiment. The conditions tested were single injection of blank hydrogel (◆), single bolus injection of 1.2 mg of GCSF dissolved in PBS (●), single injection of 1.2 mg of GCSF encapsulated within the hydrogel (★) and four bolus injections of 0.3 mg of GCSF dissolved in PBS (◆) daily. Initial injections were given on day 0 and daily injections were continued to day 3. Injection of GCSF significantly increased the number of cells mobilized into circulation, but the time periods with sustained elevated cell number were mediated by the method of administering GCSF. (b) The number of CD31+ cells mobilized on day 4 was therefore dependent on the method of administering GCSF. The conditions investigated were: single injection of blank hydrogel, single bolus injection of 1.2 mg of GCSF dissolved in PBS, single injection of 1.2 mg of GCSF encapsulated within the hydrogel and four daily bolus injections of 0.3 mg of GCSF dissolved in PBS. (c) Circulating mononuclear cells were collected four days after initial injections and expanded in endothelial growth medium *in vitro* over three passages. Cells expressing CD31, CD34, or both were identified using flow cytometry. The conditions were (i) daily bolus injections of 0.3 mg of GCSF for four days, (ii) single injection of blank hydrogel, and (iii) single injection of 1.2 mg of GCSF encapsulated within the hydrogel. The condition with administration of GCSF-encapsulating hydrogel resulted in the largest fraction of culture-expanded cells expressing CD31 and CD34 as compared with other conditions.

of the G-CSF-encapsulated hydrogels elevated the number of mononuclear cells in circulation one day after administration, and the number of cells was significantly greater than blank hydrogels without drug (Fig. 5a). The elevated mononuclear cell number was retained for 48 h followed by a gradual decrease over another 48 h. In contrast, bolus injection of the same dose of G-CSF elevated the cell number one day after injection, with drastic decrease thereafter. Repeated daily injections of G-CSF for four days maintained an elevated mononuclear cell number over the same time period with a rapid decrease after the final day of injection.

The fraction of the CD31-expressing stem and progenitor cells in the mononuclear cells was further quantified using flow cytometry. The mononuclear cells examined herein were collected on Day 4. The use of G-CSF-encapsulating PEGDA-PEI hydrogels resulted in a larger number ratio between the CD31+ cells and the mononuclear cells than a single bolus injection of G-CSF (Fig. 5b). The mononuclear cells collected on Day 4 were further cultured in endothelial growth medium to isolate and expand endothelial progenitor cells (EPCs) (Fig. 5c). Interestingly, *in vitro* expansion of mononuclear cells mobilized with G-CSF-encapsulating hydrogels produced a larger number of cells expressing CD34 and CD31 antigens, markers of EPCs, as compared with mononuclear cells mobilized via single or repeated bolus injections of G-CSF.

This result suggests that the stiff and metastable PEGDA-PEI hydrogels improved the efficacy of G-CSF for mobilizing stem and progenitor cells. It is known that G-CSF releases stem and progenitor cells residing in the bone marrow by limiting the expression of chemokines involved in cell adhesion (e.g. stromal-cell derived factor 1) and also by stimulating the monocytes' expression of matrix metalloproteinase [23]. Because the G-CSF administered into circulation has a half-life of 2–4 h, the hydrogel could have a stabilizing effect on the G-CSF, thus allowing for sustained mobilization as compared with the single bolus injection of G-CSF. Furthermore, the largest yield of CD34+ and CD31+ EPCs obtained from mononuclear cells mobilized with the G-CSF-encapsulating hydrogel implies that sustained G-CSF delivery enables stem and progenitor cell mobilization while minimally stimulating inflammatory cells. Conversely, bolus administration of G-CSF significantly increased the number of inflammatory cells including neutrophils, monocytes, B cell, and dendritic cells in circulation [24]. However, the underlying mechanism for the enhanced efficiency of stem and progenitor cell mobilization needs to be studied more thoroughly in future studies.

4. Conclusion

Overall, the results of this study demonstrate that the stiff and metastable PEGDA-PEI hydrogels allowed the decoupled control of degradation rates and stiffness. This hydrogel system was successfully used as an injectable drug delivery system enabling sustained mobilization of stem and progenitor cells into circulation. The unique stiffness of the hydrogel was attained from the highly branched architecture of PEI and the decoupled controllability of degradation rate was achieved by tuning the number of protonated amine groups of the hydrogel. We therefore expect that the degradation rates of the hydrogels developed in this study may be further controlled over a broader range through chemical modification of PEI in the hydrogel.

Acknowledgements

This work was funded by National Institute of Health (NIH 1 R21 HL097314 A), US Army Grant (W81XWH-08-1-0701) and the Illinois Regenerative Medicine Institute. Tor Jensen was funded by a Fellowship from Carle Foundation Hospital. The authors also wish

to thank Chet Utterback at the University of Illinois Poultry Research Farm (Urbana, IL) for the supply of embryonic chicken eggs.

Appendix

Figures with essential color discrimination. Figs. 1–5 and Scheme 1 in this article are difficult to interpret in black and white. The full color images can be found in the online version, at doi:10.1016/j.biomaterials.2010.11.021.

Appendix. Supplementary data

Supplementary data related to this article can be found online at doi:10.1016/j.biomaterials.2010.11.021.

References

- [1] Sheridan W, Begley C, Juttner C, Szer J, Bik To L, Maher D, et al. Effect of peripheral blood progenitor cells mobilised by filgrastim (G-CSF) on platelet recovery after high-dose chemotherapy. *Lancet* 1991;339(8794):640–4.
- [2] Kang HJ, Kim HS, Zhang SY, Park KW, Cho HJ, Koo BK, et al. Effects of intra-coronary infusion of peripheral blood stem-cells mobilised with granulocyte-colony stimulating factor on left ventricular systolic function and restenosis after coronary stenting in myocardial infarction: the MAGIC cell randomised clinical trial. *Lancet* 2004;363(9411):751–6.
- [3] Wollert K, Drexler H. Clinical applications of stem cells for the heart. *Circ Res* 2005;96(2):151–63.
- [4] Kotto-Kome AC, Fox SE, Lu W, Yang BB, Christensen RD, Calhoun DA. Evidence that the granulocyte colony-stimulating factor (G-CSF) receptor plays a role in the pharmacokinetics of G-CSF and PegG-CSF using a G-CSF-R KO model. *Pharmacol Res* 2004;50(1):55–8.
- [5] Layman H, Sacasa M, Murphy AE, Murphy AM, Pham SM, Andreopoulos FM. Codelivery of FGF-2 and G-CSF from gelatin-based hydrogels as angiogenic therapy in a murine critical limb ischemic model. *Acta Biomater* 2009;5(1):230–9.
- [6] Kong HJ, Alsborg E, Kaigler D, Lee KY, Mooney DJ. Controlling degradation of hydrogels via the size of crosslinked junctions. *Adv Mater* 2004;16(21):1917–21.
- [7] Cha C, Kim SY, Cao L, Kong H. Decoupled control of stiffness and permeability by a cell-encapsulating poly(ethylene glycol) dimethacrylate hydrogel. *Biomaterials* 2010;31(18):4864–71.
- [8] Gong J, Katsuyama Y, Kurokawa T, Osada Y. Double-network hydrogels with extremely high mechanical strength. *Adv Mater* 2003;15(14):1155–8.
- [9] Tang Q, Sun X, Li Q, Wu J, Lin J. A simple route to interpenetrating network hydrogel with high mechanical strength. *J Colloid Interface Sci* 2009;339(1):45–52.
- [10] Okumura Y, Ito K. The polyrotaxane gel: a topological gel by figure-of-eight cross-links. *Adv Mater* 2001;13(7):485–7.
- [11] Haraguchi K, Takehisa T, Fan S. Effects of clay content on the properties of nanocomposite hydrogels composed of poly(N-isopropylacrylamide) and clay. *Macromolecules* 2002;35(27):10162–71.
- [12] Ceylan D, Okay O. Macroporous polyisobutylene gels: a novel tough organogel with superfast responsiveness. *Macromolecules* 2007;40(24):8742–9.
- [13] Ritger P, Peppas N. A simple equation for description of solute release II. Fickian and anomalous release from swellable devices. *J Control Release* 1987;5(1):37–42.
- [14] Alfrey T, Gurnee EF, Lloyd WG. Diffusion in glassy polymers. *J Polym Sci Polym Symp* 1966;12(1):249–61.
- [15] Korsmeyer R, Peppas N. Macromolecular and modeling aspects of swelling controlled system in controlled release delivery systems. In: Kydonieus AF, editor. *Treatise on controlled drug delivery: fundamentals, optimization, applications*. New York: Marcel Dekker; 1992. p. 196.
- [16] Quijada-Garrido I, Prior-Cabanillas A, Garrido L, Barrales-Rienda J. Swelling monitoring of poly[(N-isopropylacrylamide)-co-(methacrylic acid)] copolymers by magnetic resonance imaging. *Macromolecules* 2005;38(17):7434–42.
- [17] Tritt-Goc J, Kowalczyk J, Piślewski N. MRI study of Fickian, case II and anomalous diffusion of solvents into hydroxypropylmethylcellulose. *Appl Magn Reson* 2005;29(4):605–15.
- [18] Lee H, Jhon Andrade J. Nature of water in synthetic hydrogels. I. Dilatometry, specific conductivity, and differential scanning calorimetry of poly-hydroxyethyl methacrylate. *J Colloid Interface Sci* 1975;51(2):225–31.
- [19] Zijlstra A, Mikolon D, Stupack DG. Angiogenesis assays in the chick. In: Staton C, Lewis CE, Bicknell RJ, Bicknell R, editors. *Angiogenesis assays: a critical appraisal of current techniques*. J. Wiley & Sons; 2007. p. 183.

- [20] Lutolf M, Hubbell J. Synthesis and physicochemical characterization of end-linked poly(ethylene glycol)-co-peptide hydrogels formed by Michael-type addition. *Biomacromolecules* 2003;4(3):713–22.
- [21] Koyama Y, Yamashita M, Iida-Tanaka N, Ito T. Enhancement of transcriptional activity of DNA complexes by amphoteric PEG derivative. *Biomacromolecules* 2006;7(4):1274–9.
- [22] Mao S, Neu M, Germershaus O, Merkel O, Sitterberg J, Bakowsky U, et al. Influence of polyethylene glycol chain length on the physicochemical and biological properties of poly(ethylene imine)-graft-poly(ethylene glycol) block copolymer/SiRNA polyplexes. *Bioconjug Chem* 2006;17(5):1209–18.
- [23] Lemoli RM, D'Addio A. Hematopoietic stem cell mobilization. *Haematologica* 2008;93(3):321–4.
- [24] Buzzeeo MP, Yang J, Casella G, Reddy V. Hematopoietic stem cell mobilization with GCSF induces innate inflammation yet suppresses adaptive immune gene expression as revealed by microarray analysis. *Exp Hematol* 2007;35(9):1456–65.